ChemComm

Dithiol-based Modification of Poly(dopamine): Enabling Protein Resistance via Short-Chain Ethylene Oxide Oligomers

Journal:	*ChemComm*
Manuscript ID:	CC-COM-01-2015-000299.R1
Article Type:	Communication
Date Submitted by the Author:	20-Feb-2015

Complete List of Authors:	Vaish, Amit; National Institute of Standards and Technology, NCNR Walker, Marlon; National Institute of Standards and Technology, Material Measurement Laboratory Steffens, Kristen; National Institute of Standards and Technology, Material Measurement Laboratory Vanderah, David; National Institute of Standards and Technology, Institute for Bioscience and Biotechnology Research Richter, Lee; National Institute of Standards and Technology, Materials Mesaurment Laboratory Dimitriou, Michael; National Institute of Standards and Technology, NCNR

ChemComm

RSCPublishing

COMMUNICATION

Dithiol-based Modification of Poly(dopamine): Enabling Protein Resistance via Short-Chain Ethylene Oxide Oligomers

Cite this: DOI: 10.1039/x0xx00000x

Received 00th January 2015,
Accepted 00th January 2015

DOI: 10.1039/x0xx00000x

www.rsc.org/

Amit Vaish[a,d]*, David J. Vanderah[b,c], Lee J. Richter[b], Michael Dimitriou[a], Kristen L. Steffens[b] and Marlon L. Walker[b]*

We present a facile strategy to modify poly(dopamine)(PDA)-coated substrates. Using thiol-terminated short chain ethylene oxide oligomers (OEG) under aqueous conditions, we explore the creation of a model surface exhibiting resistance to nonspecific protein absorption (RPA) by engineering the surface properties of a PDA adlayer. Surprisingly, dithiol-terminated OEG molecules demonstrated significantly greater coverage on PDA surfaces than analogous monothiol molecules. Successful RPA is only achieved with dithiol-terminated OEGs.

Biologically-inspired adhesives and coatings have become increasingly popular for modifying surfaces of organic and inorganic materials in various technical and biomedical applications.[1,2] One such compound, poly(dopamine) (PDA), developed as a mimic to the mussel adhesive protein,[3] is emerging as a universal coating material, capable of adhering to a wide array of surfaces such as metals, ceramics, and polymers.[4,5] PDA is synthesized by the condensation of dopamine, a catecholamine, in water under alkaline solution conditions. The aggregates readily deposit on surfaces upon contact to form a thin film of controllable thickness.[3] A distinct advantage of a PDA coating is that surface properties can be tailored by further functionalization. "As prepared" PDA films nonspecifically adsorb protein readily, regardless of the characteristics of the underlying substrate.[6,7] Imparting the property of high resistance to protein adsorption (RPA) is essential for exploiting the potential usefulness of incorporation of PDA-coated substrates into various medical/biotechnological devices to overcome failures due to fouling (e.g., biofilm formation on implants such as stents) or impeded operation (e.g., spurious signals in biosensors or heart pacemakers).[8] Recent studies have demonstrated high RPA of modified PDA surfaces following polymer functionalization by 'grafting from' or 'grafting to' approaches.[7,9,10] Although successful, these strategies are plagued with either tedious surface-initiated atom transfer radical polymerization reactions or requirement of elevated temperatures during poly(ethylene) glycols immobilization for achieving optimal polymer grafting density. In distinct contrast, surface modification via self-assembly of small molecules onto coinage metals (i.e., thiols on Au and Ag) and oxidic surfaces (e.g., phosphonates and silanes on SiO_2) is a well-established, facile approach.[11,12] We, and others, have demonstrated high RPA on Au using small oligomers of ethylene glycol-terminated thiols.[13-15] Herein, we present a detailed characterization of small organosulfur compound attachment to PDA and explore the possibility of creating protein-resistant PDA surfaces with oligo(ethylene glycol) [OEG] compounds without the need for elevated temperatures. In particular, we report on the structure and coverage of octadecanethiol (ODT), monothiol- (MTOEG), and dithiol-based (DTOEG) OEG self-assembled monolayers (SAMs) on PDA (Figure 1A). A SAM of the dithiol **(3)** on Au substrates has been shown to exhibit high RPA to both blood serum and membrane proteins.[16]

Despite numerous attempts to describe the chemical structure of surface-adherent PDA films there still is no general consensus about either PDA structure or the molecular mechanism behind PDA formation. It is generally described as a conglomerate of quinones, indoles, and catechols in the form of dimers and oligomers, held together by covalent bonds, π stacking, and hydrogen bonds[17,18] Additionally, it has been observed that the thickness of the deposited PDA film can be tuned by controlling the time the substrate is in contact with the alkaline dopamine solution.[3,19] We employed multiple techniques including X-ray photoelectron spectroscopy (XPS), X-ray reflectivity (XRR), and spectroscopic ellipsometry (SE) for a detailed physiochemical characterization of the surface modification of PDA films (experimental details are in †ESI). The high-resolution XPS spectra acquired for PDA indicate not only the presence of chemical groups of monomeric dopamine (i.e., C-O, $C_{Aromatic}$ ($\pi \rightarrow \pi^*$), C-C, and R-NH_2),[20] but also include additional functionalities (i.e., C=O, R_2NH) attributed to indolequinones and other intermediates as previously reported (Figure 1B).[17-21] The small substrate Si peak (< 2%) in the XPS spectra indicates that the PDA films are likely continuous with thickness on the order of the XPS sampling depth (~10 nm).[3,22] Figure 1C shows the XRR profile of a PDA film as a function of Q, the momentum transfer normal to the surface ($Q= 4\pi \sin\Theta/\lambda$, where Θ is the incident angle and λ is the wavelength of the incident X-ray beam). The solid blue line represents a best-fit curve based on a three layer PDA-SiO_2-Si model. The subsequent X-ray scattering length density (SLD) profiles (Figure 1C)

were derived from fits to the model. Complete surface coverage of the SiO_2-Si by PDA was deduced from the fact that the fitted PDA SLD, 1.39 x 10^{-5} Å^{-2}, is close to the theoretical PDA SLD of 1.17 x 10^{-5} Å^{-2} (†ESI). Additionally, the XRR data fits indicate a PDA film thickness of (13.2 ± 0.8) nm with (3.1 ± 0.4) nm interfacial roughness.[23,24]

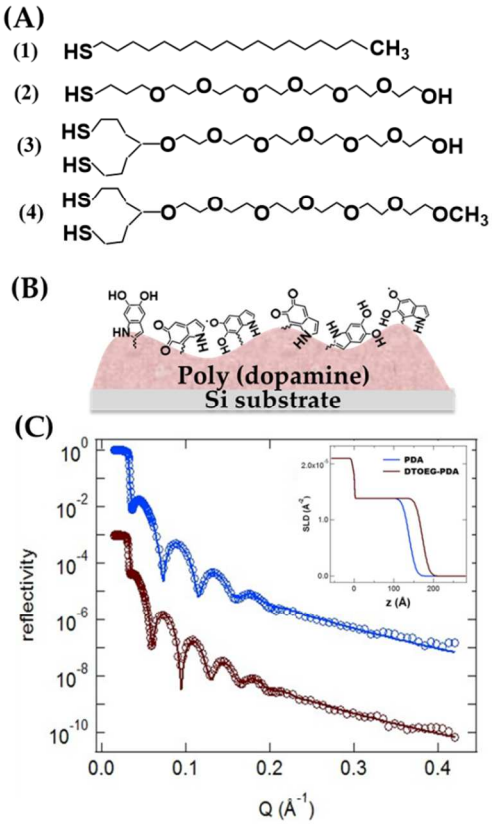

Figure 1. (A) Monothiol and dithiol compounds used; (**1**) octadecanethiol (**ODT**), (**2**) 1-mercaptopropyl-hexa(ethylene glycol) (**MTOEG**), (**3**) 1-(3′-mercaptopropyloxy)-hexa(ethylene glycol) (**DTOEG**), and (**4**) 1-(1′,7′-dimercaptoheptyl-4′-oxy)-17-methoxy)-hexa(ethylene glycol). **(B)** Schematic illustration of a probable physiochemical structure of poly (dopamine) (PDA) film on Si substrate, **(C)** X-ray reflectivity (XRR) (data represented by circular symbols, best-fitted curves are represented by solid lines, and curves are offset for clarity) and corresponding scattering length density (SLD) profiles of PDA film before (blue) and after DTOEG functionalization (brown).

We also characterized the thin PDA films using SE to complement the XRR measurements. Our SE (*ex situ*) data denote PDA film thickness of (14.2 ± 2.1) nm, in good agreement with the XRR measurements. Atomic force microscopy (AFM) scans illustrate a granular PDA film with randomly distributed PDA aggregates (†ESI). Additionally, AFM measurements confirm the roughness of the film indicated by XRR, and reveal an interfacial root-mean-squared roughness of (4.6 ± 2.5) nm. Previous studies also reported similar topography of PDA films[4,10,25] suggesting that this level of roughness is an intrinsic characteristic of these films.

It is well known that alkanethiols interact with Au substrates and self-assemble into a one molecule thick layer (Figure 2A).[11,12] We investigated thiol modification of PDA surfaces using ODT (Figure 1A(**1**)) as a model system, employing XPS, SE, and sessile drop water contact angle (CA) measurements to characterize the ODT-modified PDA, and compare these findings to those for ODT on Au. As shown in the XPS spectrum for sulfur (S 2p, Figure 2B), ODT on Au exhibited a well-defined doublet peak of the thiolate bond (C-S-Au) starting at 161.8 eV.[11] In contrast, the XPS S 2p spectra from ODT-on-PDA exhibited a doublet peak at 163.3 eV, indicating the formation of a thioether (C-S-C) bonds[26] between the sulfur atom of ODT and the PDA layer[27] possibly via the previously hypothesized Michael addition reactions with quinone moieties (Figure 2C).[28]

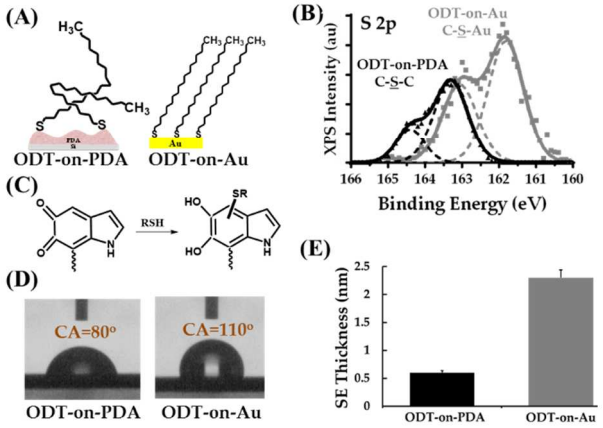

Figure 2. (A) Schematic illustration of ODT-on-PDA and –on-Au, **(B)** XPS S 2p spectra of ODT-on-PDA (black line) and –on-Au (grey line), spectra were fitted with Gaussian-Lorentzian line shapes (broken lines) for binding energies contribution at S $2p_{1/2}$ and S $2p_{3/2}$ with an area ratio of 2:1 and binding energy difference of 1.2 eV, **(C)** Michael-addition thiol-on-PDA structures , **(D)** sessile contact angle (CA) snapshots of ODT-on-PDA and ODT-on-Au, and **(E)** spectroscopic ellipsometry (SE) thicknesses of ODT-on-PDA and ODT-on-Au.

Contact angle (CA) data (Figure 2D) and SE measurements (Figure 2E) suggest significantly less ODT on the PDA layer compared to Au. The SE thickness of ODT on PDA (0.6 ± 0.1) nm is ~ 4 times less than the ODT on Au (2.3 ± 0.2) nm, corresponding to approximate ODT interfacial mass densities of 66 ng/cm^2 and 2.5 x 10^2 ng/cm^2, respectively. $CA_{(ODT\text{-}on\text{-}PDA)}$ (80 ± 6)^o is also lower than $CA_{(ODT\text{-}on\text{-}Au)}$ (110 ± 3)^o. Previous studies on octadecyltrichlorosilane (OTS)-SiO_2-Si SAMs have shown that incomplete ODT coverage results in lower wettabilities (CA ≈ 90^o).[29] We attribute the intermediate wettability of ODT-functionalized PDA to low ODT coverage, possibly resulting in both exposed areas (no thiols bound) of the more wettable PDA [CA=(35 ± 5)^o] and disordered surface-bound ODT molecules (Figure 2A). Our structural assessment of ODT on our surfaces is in contrast to the initial report on alkanethiol modification of PDA (Lee *et al.*), who described dodecanethiol (DDT)-on-PDA as a pseudo-SAM on the basis of CA measurements.[3] However, it may have been overlooked that the $CA_{(DDT\ on\ PDA)}$ was ≈ 20^o less than that of well-ordered DDT SAMs on Au (118^o).[30,11,31]

We functionalized PDA to evaluate RPA with small OEG compounds using MTOEG **(2)**, similar to previous OEG compounds known to engender protein resistance on Au substrates[14], and DTOEG **(3)** – a new dithiol analog of the previous bissulfur (bisthiolacetate) OEG, N,N(bis3'thioacetylpropyl)-3,6,9,12,15,18 hexaoxanonadecanamide, BTHA[15] (Figure 1A). The position of the signal in the S 2p region of XPS spectra indicates that both the

MTOEG and DTOEG are bound to the PDA via thioether (C-S-C) bonds (B.E. 163.3 eV) [Figure 3A], as expected. Thiol coverage, estimated from the areas under the S 2p peaks, indicates the surface density of DTOEG as ≈ 25 times higher than that of MTOEG (inset Figure 3A). Film thickness increases from SE and XRR data support the surprisingly large differential surface modification by DTOEG indicated in the XPS data. The thickness increase after DTOEG functionalization, by SE (4.2±0.6) nm (Figure 3B) and XRR (3.7 ± 0.4) nm (Figure 1C), is significantly higher than that for MTOEG, SE = (0.4±0.2) nm. From the SE data we calculated approximate interfacial mass densities of 4.6×10^2 ng/cm^2 (DTOEG) and 44 ng/cm^2 (MTOEG) on PDA. The higher interfacial mass density achieved with dithiols maybe a general phenomenon as modification with an alternative, methyl terminated dithiol OEG molecule[16] (Figure 1C **(4)**) results in ellipsometric thickness on PDA (4.4 nm) similar to that of DTOEG.

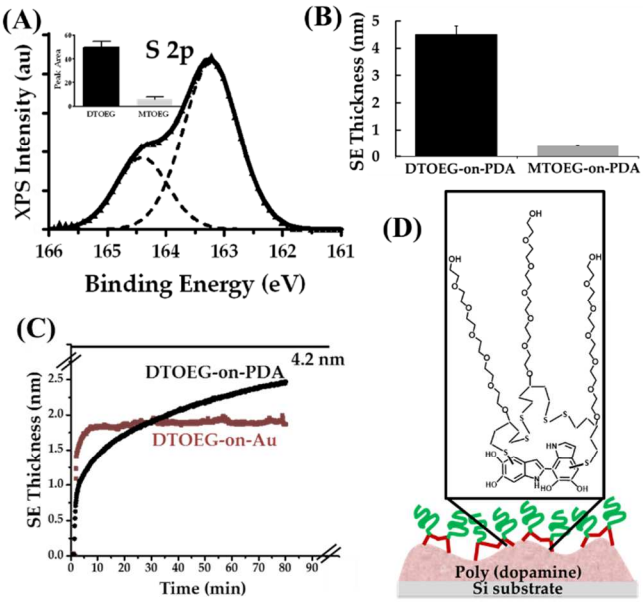

Figure 3. (A) XPS S 2p spectrum of DTOEG (black solid line) on PDA was fitted with Gaussian-Lorentzian line shape (broken lines) for binding energy contributions at S $2p_{1/2}$ and S $2p_{3/2}$ with an area ratio of 2:1 and binding energy difference of 1.2 eV, and inset shows quantification of corresponding S 2p areas under the peak, **(B)** SE thickness of DTOEG and MTOEG on PDA substrates, **(C)** adsorption profiles of DTOEG on Au (brown) and on PDA (black) and the horizontal black line represents the maximum obtained SE thickness of DTOEG on PDA surfaces, and **(D)** schematic illustration of DTOEG attachment on PDA by a probable disulfide-mediated DTOEG multilayer structure formation.

The SE thickness increase after MTOEG functionalization on PDA, (0.4 ± 0.2) nm (Figure 3B), is significantly lower than MTOEG SAMs on Au, (1.3 ± 0.08) nm,[14] analogous to the lower SE thickness found for ODT on PDA vs. Au (Figure 2E). In contrast, the SE thickness increase after DTOEG functionalization on PDA, (4.2 ± 0.5) nm is strikingly higher than DTOEG SAMs on Au, (1.8 ± 0.19) nm. Additionally, adsorption rates of DTOEG on Au and PDA are significantly different (Figure 3C). A rapid initial adsorption is observed on Au, attaining 90% of the maximum SE thickness (1.8 ± 0.19) nm in ~ 10 min. In contrast on PDA, a significantly slower adsorption is observed, requiring ~ 6 h to attain the maximum SE thickness increase [(4.2 ± 0.5) nm]. This DTOEG thickness increase is larger than expected for a simple monolayer on the basis of the number of atoms in the molecule [24] from the sulfur (HS group) to the oxygen (terminal OH group)]. Although a definitive structural model of DTOEG-on-PDA remains to be established, we conjecture the possibility of a DTOEG multilayer structure formation via *in-situ* oligomerization of DTOEG molecules (Figure 3D). As mentioned earlier that during PDA synthesis, oxidation of dopamine results into multiple intermediate species comprising indole in different oxidation states.[32] One such intermediate species, semiquinone, has been recently demonstrated by electron paramagnetic resonance spectroscopy to be present in the PDA samples.[33] Additionally, previous studies have illustrated that semiquinone radicals can transform thiols into thiyl radicals by abstraction of a hydrogen atom.[34] Based on these studies, we hypothesized that the presence of semiquinone radicals in PDA films might also have an influence in the thiol attachment process on PDA. In particular, DTOEG, due to the presence of two thiol moieties on a molecule, may have multiple reaction pathways available for PDA-mediated interactions, yielding products such as thioether bond with randomly distributed indolequinones on PDA by the aforementioned Michael-addition, semiquinone-mediated DTOEG oligomeric species containing disulfide bonds[34] or thiyl radical formation at the PDA/solution interface (details are in †ESI). We propose that DTEOG-on-PDA is comprised of small oligomers of DTOEG in which a DTOEG molecule is chemically attached to the PDA surface via a thioether bond, and the other thiol moiety is subsequently linked to DTOEG through disulfide bonds (Figure 3D). In a preliminary experiment to test for the presence of the disulfide-mediated DTOEG multilayer structure, we introduced a disulfide bond reducing agent, tris(2-carboxyethyl)phosphine (TCEP) [50 mM solution] to a DTOEG-on-PDA surface. We observed a significant drop in the DTOEG thickness to less than a simple monolayer thickness within 10 min, suggesting degradation in the DTOEG multilayer due to reduction of the disulfide linkage.

In order to probe the protein resistance of our OEG-functionalized-PDA surfaces, we used fibrinogen (Fb), a rod-shaped blood plasma protein, as a model protein. As shown in Figure 4, protein adsorption on MTOEG-derivatized and non-derivatized PDA surfaces are similar. This suggests that the low interfacial mass density of MTOEG (44 ng/cm^2) results in exposed PDA areas, allowing direct protein-PDA contact and adsorption (Figure 4A upper schematic).[6] In contrast, the DTOEG-derivatized PDA shows significantly higher RPA to Fb (~ 3% binding response as compared to that on non-derivatized PDA surfaces). Additionally, DTOEG-on-PDA exhibits excellent RPA to fetal bovine serum (FBS, a complex mixture of proteins), ≈10% binding response as compared to that on non-derivatized PDA surfaces. The ultra-low adsorbed amount of FBS [(26 ± 4) ng/cm^2] is comparable to that previously reported for the higher molecular weight PEG functionalization.[7,10,35] We further explored the DTOEG functionalization by Fb-mediated PDA substrate screening. As illustrated in Figure 4B, Fb adsorption decreases linearly with increasing DTOEG mass density on the PDA, tuned by varying the immersion times of the PDA in the DTOEG solution [Figure 3C, maximum mass density (final SE thickness) obtained at longer immersion times (> 6 h)]. Moreover, aforementioned TCEP-reduced DTOEG-functionalized PDA surface lost its protein-resistant property when exposed to Fb. Therefore, the high RPA of the DTOEG-functionalized-PDA is attributed to effective screening of underlying PDA (Figure 4A lower schematic) due to the higher surface coverage enabled by the dithiol attachment (Figure 3D).

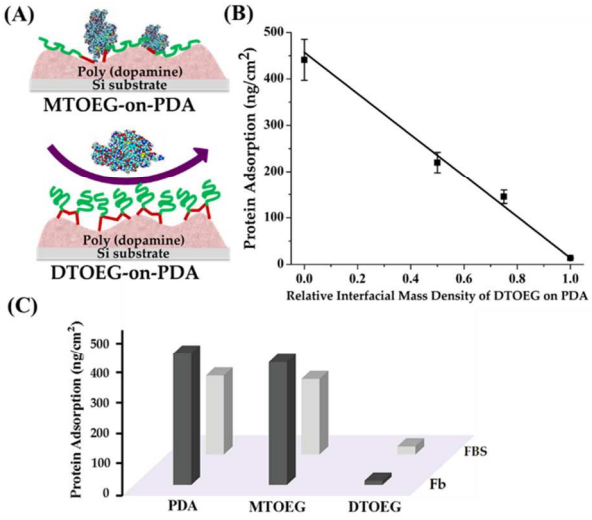

Figure 4. (A) Schematic illustration of protein interaction with MTOEG and DTOEG on PDA surfaces, **(B)** plot of Fibrinogen (Fb) adsorption as a function of DTOEG interfacial mass density on PDA surfaces (mass densities were normalized by dividing with maximum mass density of DTOEG on PDA, and the solid line represents the linear fit of the experimental data), and **(C)** *in situ* SE protein adsorption studies using Fb and fetal bovine serum (FBS) on PDA with and without thiols (MTOEG, DTOEG) modification. The standard deviations are ~5% of the mean for all conditions.

We have developed a straightforward method for creating functional materials based on substrate-independent PDA modification followed by thiol functionalization and have demonstrated the fabrication of protein-resistant surfaces using small organic compounds at room temperature under aqueous conditions. We conclusively show that small monothiols [$HS(CH_2)_3R$, where R = an oligo(ethylene glycol) segment] do not attain sufficiently high mass density on PDA to provide protein adsorption resistance. However, simply modifying the functionalizing approach to employ compounds with a dithiol motif [$(HS(CH_2)_3)_2CHR$] results in adequate coverage/screening of the underlying PDA. Expanding the substantial library of small organosulfur compounds, now commercially available for surface modification, to the dithiol motif may empower PDA functionalization for diverse applications.[12,36] Future efforts will be directed towards developing an understanding of the higher dithiols coverage and oligomerization on PDA substrates, and extending the scope of PDA functionalization for the fabrication of biomimetic constructs such as solid-supported bilayer and tethered-lipid bilayer membranes.[37,38]

Notes and references

A.V. acknowledge the National Institute of Standards and Technology-American Recovery and Reinvestment Act (NIST-ARRA) fellowship to support this work.

[a] *NIST Center for Neutron Research*
[b] *Materials Measurement Laboratory, NIST*
[c] *Institute for Bioscience and Biotechnology Research, National Institute of Standards and Technology, Rockville, MD 20850*
National Institute of Standards and Technology, Gaithersburg, Maryland 20899-8313
E-mail: anv@udel.edu, marlon.walker@nist.gov
[d] *Department of Chemical and Biomolecular Engineering, University of Delaware, Newark, Delaware, 19716*

† Electronic Supplementary Information (ESI) available

(1) B. P. Lee, P. B. Messersmith, J. N. Israelachvili, J. H. Waite *Annu. Rev. Mater. Res.* 2011, **41**, 99.
(2) C. E. Brubaker, P. B. Messersmith *Langmuir* 2012, **28**, 2200.
(3) H. Lee, S. M. Dellatore, W. M. Miller, P. B. Messersmith *Science* 2007, **318**, 426.
(4) A. Rai, C. C. Perry *J. Mater. Chem.* 2012, **22**, 4790.
(5) Y. Liu, K. Ai, L. Lu *Chem. Rev.* 2014, **114**, 5057.
(6) T. A. Morris, A. W. Peterson, M. J. Tarlov *Anal. Chem.* 2009, **81**, 5413.
(7) O. Pop-Georgievski, D. Verreault, M.-O. Diesner, V. Proks, S. Heissler, F. Rypáček, P. Koelsch *Langmuir* 2012, **28**, 14273.
(8) J. M. Anderson *Annu. Rev. Mater. Res.* 2001, **31**, 81.
(9) A. Lokanathan, S. Zhang, V. Regina, M. Cole, R. Ogaki, M. Dong, F. Besenbacher, R. Meyer, P. Kingshott *Biointerphases* 2011, **6**, 180.
(10) O. Pop-Georgievski, S. t. p. n. Popelka, M. Houska, D. Chvostová, V. r. Proks, F. e. Rypáček *Biomacromolecules* 2011, **12**, 3232.
(11) A. Ulman *Chem. Rev.* 1996, **96**, 1533.
(12) J. C. Love, L. A. Estroff, J. K. Kriebel, R. G. Nuzzo, G. M. Whitesides *Chem. Rev.* 2005, **105**, 1103.
(13) P. Harder, M. Grunze, R. Dahint, G. M. Whitesides, P. E. Laibinis *J. Phys. Chem. B* 1998, **102**, 426.
(14) A. Vaish, V. Silin, M. L. Walker, K. L. Steffens, S. Krueger, A. A. Yeliseev, K. Gawrisch, D. J. Vanderah *Chem. Commun.* 2013, **49**, 2685.
(15) D. J. Vanderah, R. J. Vierling, M. L. Walker *Langmuir* 2009, **25**, 5026.
(16) A. Vaish, D. J. Vanderah, R. Vierling, F. Crawshaw, D. T. Gallagher, M. L. Walker *Colloids Surf. B.* 2014, **122**, 552.
(17) R. A. Zangmeister, T. A. Morris, M. J. Tarlov *Langmuir* 2013, **29**, 8619.
(18) J. Liebscher, R. Mrówczyński, H. A. Scheidt, C. Filip, N. D. Hădade, R. Turcu, A. Bende, S. Beck *Langmuir* 2013, **29**, 10539.
(19) F. Bernsmann, A. Ponche, C. Ringwald, J. Hemmerlé, J. Raya, B. Bechinger, J.-C. Voegel, P. Schaaf, V. Ball *J. Phys. Chem. C* 2009, **113**, 8234.
(20) M. B. Clark, J. A. Gardella, T. M. Schultz, D. G. Patil, L. Salvati *Anal. Chem.* 1990, **62**, 949.
(21) D. R. Dreyer, D. J. Miller, B. D. Freeman, D. R. Paul, C. W. Bielawski *Langmuir* 2012, **28**, 6428.
(22) H. Hu, A. H. Carim *J. Electrochem. Soc.* 1993, **140**, 3203.
(23) J. Koo, S. Park, S. Satija, A. Tikhonov, J. C. Sokolov, M. H. Rafailovich, T. Koga *J. Colloid Interface Sci.* 2008, **318**, 103.
(24) L. C. C. Elliott, B. Jing, B. Akgun, Y. Zhu, P. W. Bohn, S. K. Fullerton-Shirey *Langmuir* 2013, **29**, 3259.
(25) F. Bernsmann, O. Ersen, J.-C. Voegel , E. Jan, N. A. Kotov, V. Ball *ChemPhysChem* 2010, **11**, 3299.
(26) H. M. Zareie, C. Boyer, V. Bulmus, E. Nateghi, T. P. Davis *ACS Nano* 2008, **2**, 757.
(27) J. A. Gardella, S. A. Ferguson, R. L. Chin *Appl. Spectrosc.* 1986, **40**, 224.
(28) Y. J. Abul-Hajj, K. Tabakovic, W. B. Gleason, W. H. Ojala *Chem. Res. Toxicol.* 1996, **9**, 434.
(29) D. H. Flinn, D. A. Guzonas, R. H. Yoon *Colloids Surf., A* 1994, **87**, 163.
(30) P. E. Laibinis, G. M. Whitesides, D. L. Allara, Y. T. Tao, A. N. Parikh, R. G. Nuzzo *J. Am. Chem. Soc.* 1991, **113**, 7152.
(31) C. D. Bain, G. M. Whitesides *Angew. Chem. Int. Ed. Engl.* 1989, **28**, 506.
(32) J. Yang, M. A. Cohen Stuart, M. Kamperman *Chem. Soc. Rev.* 2014, **43**, 8271.
(33) N. F. Della Vecchia, A. Luchini, A. Napolitano, G. D'Errico, G. Vitiello, N. Szekely, M. d'Ischia, L. Paduano *Langmuir* 2014, **30**, 9811.
(34) J.-M. Richard, D. Cantin-Esnault, A. Jeunet *Free Radical Biol. Med.* 1995, **19**, 417.
(35) T. Riedel, Z. Riedelová-Reicheltová, P. Májek, C. Rodriguez-Emmenegger, M. Houska, J. E. Dyr, E. Brynda *Langmuir* 2013, **29**, 3388.
(36) M. E. Lynge, R. van der Westen, A. Postma, B. Stadler *Nanoscale* 2011, **3**, 4916.
(37) V. Früh, A. P. Ijzerman, G. Siegal *Chem. Rev.* 2010, **111**, 640.
(38) R. Budvytyte, G. Valincius, G. Niaura, V. Voiciuk, M. Mickevicius, H. Chapman, H.-Z. Goh, P. Shekhar, F. Heinrich, S. Shenoy, M. Lösche, D. J. Vanderah *Langmuir* 2013, **29**, 8645.

